Exploring the Optical Properties of Holey Fibres

Tanya M. Monro, N.G. Broderick and D.J. Richardson

Optoelectronics Research Centre, University of Southampton SO171BJ United Kingdom

Abstract. The novel optical properties of holey optical fibres are reviewed, and a complete hybrid vector model for these structures is described.

INTRODUCTION

A new class of optical fibre has emerged in the last few years; the *holey* or *microstructured* optical fibre. A typical holey fibre is shown in Fig. 1. The core of the fibre is formed by a solid silica region, and the cladding is comprised of air holes which run along the fibre. These new fibres have generated a great deal of interest largely because they can possess a wide range of novel optical properties which are not easily attainable in more conventional fibre types [1,2].

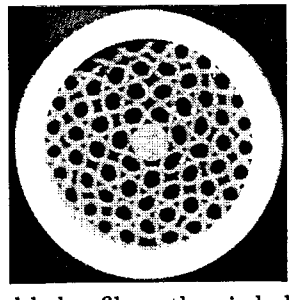

FIGURE 1. A typical holey fibre: the air holes define the cladding.

In fibres like the one shown in Fig. 1, light can be guided using either one of two quite different mechanisms. Ref. [3] originally proposed that these structures could guide light via photonic band gap effects; and this was demonstrated in Ref. [4]. The second means of guiding light in these structures makes fewer demands on the fibre geometry. In fibres like the one shown in Fig. 1, light can be guided due to an effective average index difference between the central core and the region containing air holes, which acts as the cladding. This *effective index* guidance is routinely observed in these fibres, and their basic operation does not depend on having a periodic array of holes; in fact the holes can even be arranged randomly [5]. Such fibres are generally labelled *holey fibres* (HFs) or *microstructured fibres.*

OVERVIEW OF HF PROPERTIES

The effective index difference between core and cladding (Δn) is a strong function of wavelength in a HF. At longer wavelengths, the mode extends further into the holes, thereby reducing the effective cladding index. At shorter wavelengths, the mode is tightly confined to the core, and Δn is reduced. This results in a range of novel properties for such fibres, some of which are listed below.

1. **Endless single-modedness** HFs with small air holes can be endlessly single-moded [1]. The structure remains single-mode at short wavelengths because Δn is reduced as the wavelength decreases. Such a fibre remains single-moded even if the physical dimensions of the structure are scaled.

2. **Tailorable mode size** The mode area in a HF can be tailored over three orders of magnitude by scaling the dimensions of the structure. Mode areas can from less than $1\,\mu\text{m}^2$ to over $500\,\mu\text{m}^2$ are possible [2]. The small mode fibres can be used to explore a non-linear effects [6], whereas the large mode fibres allow high power delivery [7].

3. **Tailorable mode shape** The shape of HF modes depends on the arrangement of air holes and the fibre dimensions. The mode shown in Fig. 2 reflects the hexagonal arrangement of air holes. In fibres like the one in Fig. 1, the interstitial holes can act to *circularize* the mode profile by as much as 15% [8]. This should aid the integration of these fibres with conventional fibre systems.

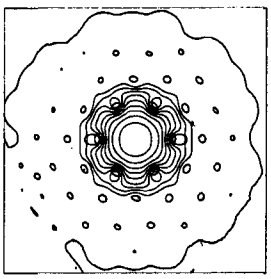

FIGURE 2. A single-mode small-core holey fibre. The guided mode @1.55 μm is superimposed.

4. **Evanescent field interaction with air** HFs open up new opportunities for exploiting the interaction of light with gases and liquids via evanescent field effects. The HF geometry can naturally provide long optical path lengths; by appropriate fibre design, up to 40% of the guided mode can be located in the holes [9]. Applications include gas sensing, nonlinear switching etc.

5. **Dispersion flattening** Holey fibres can demonstrate ultra-broadband dispersion flattening [2,10]. The dispersion slope can be $\approx 0.002\,\text{ps}\,\text{km}^{-1}\,\text{nm}^{-2}$ from $\lambda = 1.3 \rightarrow 1.6\,\mu\text{m}$ [2]. Applications include broadband WDM devices, etc.

6. **Anomalous dispersion below 1.3 microns** The zero-dispersion wavelength can be as low as 650 nm [11] in a single-mode HF, something not possible

with conventional fibres. This leads to a range of new possibilities, including: solitons in the visible, continuum generation, etc.

7. **Dispersion compensation** Particular types of HF designs can be highly dispersive, with normal dispersion values as large as -2000 ps/nm/km [12]. Such fibres could be used for dispersion compensation.

MODELLING HOLEY FIBRES

The first method which was developed to model holey fibres was the *effective index model* [1], which approximates HF using a step-index fibre with a cladding index n_{eff} equal to the effective index in the HF cladding. This approach ignores the spatial distribution of the refractive index profiles within HFs. Even so, it can provide some insight into HF operation. However this reduced model is unable to accurately predict modal properties such as the dispersion or birefringence, which depend critically on the hole configuration [15,2]. To do this a model which takes into account the complicated transverse refractive index profile is required.

One candidate approach was developed by Silvestre et al. [13] which decomposes the modal fields and the refractive index profile into plane waves, and can describe any complex spatial index distribution. However, as it does not take advantage of the localisation of the guided modes, many terms are needed for accuracy. This technique defines the refractive index in a restricted region and uses periodic boundary conditions to extend the structure. This additional periodicity restricts its applicability to HFs, which do not need to be periodic [5]. A similar approach is the variational plane-wave method in Ref. [14]. An alternate approach was developed by Mogilevtsev et al. [15] which describes the modes using localised functions. Although this technique takes advantage of mode localisation, and so is more efficient than the plane-wave methods, it cannot be accurate unless the refractive index is also represented well.

Here we describe a hybrid approach, which combines the best features of the techniques described above. In this approach the core and the air holes are described independently, so that each quantity can be represented accurately and efficiently. A scalar version of this approach was described in Ref. [2], followed by a vector implementation in Ref. [8]. In both papers, only symmetric structures and modes were considered. In order to model HFs with an asymmetric index profile or to obtain accurate predictions for the second-mode cutoff, it is necessary to extend this approach. Here we present a completely general implementation of this hybrid approach, which can be used to explore the full range of HF structures and modes.

Hybrid Orthogonal Function Model

We assume the fibre is uniform in the z-direction, so the modal electric field is

$$\mathbf{E}_j(x,y,z) = \left(\mathbf{e}_j^{\mathrm{t}}(x,y) + e_j^z(x,y)\hat{\mathbf{z}}\right) \exp\left(i\beta_j z\right) \tag{1}$$

where (x, y) is the transverse plane, β_j is the propagation constant of the j^{th} mode, and $\mathbf{e}_j^t$ and e_j^z are the transverse and longitudinal components. The transverse field is then written as $\mathbf{e}_j^t = e_x\hat{\mathbf{x}} + e_y\hat{\mathbf{y}}$. Using Eq. (1) in the vector wave equation yields the following coupled equations for the electric fields $e_x(x, y)$ and $e_y(x, y)$ [16]

$$\left[\frac{\nabla^2}{k^2} - \frac{\beta^2}{k^2} + n^2\right] e_x = \frac{-1}{k^2}\frac{\partial}{\partial x}\left(e_x\frac{\partial \ln n^2}{\partial x} + e_y\frac{\partial \ln n^2}{\partial y}\right)$$
$$\left[\frac{\nabla^2}{k^2} - \frac{\beta^2}{k^2} + n^2\right] e_y = \frac{-1}{k^2}\frac{\partial}{\partial y}\left(e_x\frac{\partial \ln n^2}{\partial x} + e_y\frac{\partial \ln n^2}{\partial y}\right) \qquad (2)$$

where $k = 2\pi/\lambda$ is the wavenumber and $n(x, y)$ is the transverse index profile. The subscript (j) has been dropped for brevity. To solve Eqs (2), we decompose the refractive index and the modal field. The choice of functions is the crucial step in making this method efficient and accurate, and they are described next.

Decompositions

The modal electric field is expanded as

$$\mathbf{e}^t(x, y) = \sum_{a,b=0}^{F-1}\left(\mathcal{E}_{ab}^x\,\psi_a^m(x)\psi_b^m(y)\,\hat{\mathbf{x}} + \mathcal{E}_{ab}^y\,\psi_a^m(x)\psi_b^m(y)\,\hat{\mathbf{y}}\right) \qquad (3)$$

where the ψ_a^m are orthonormal Hermite-Gaussian (HG) functions with a width $w_m \propto \Lambda$, where Λ is the inter-hole separation. More details are given in Ref. [2]. In this implementation, odd and even HGs are used, to allow symmetric and non-symmetric mode profiles to be calculated. Typically only a small number of terms is needed to reconstruct the observed modal profiles.

The transverse refractive index profile is described in two parts. The hole arrangement is described using a Fourier decomposition, and the central core is described using HGs of width $w_d \propto d$, where d is the hole diameter. Hence we write

$$n^2 = \sum_{a,b=0}^{C-1} c_{ab}\;\psi_a^d(x)\;\psi_b^d(y) +$$
$$\sum_{a,b=0}^{P-1}\left(p_a^c\;cos(asx) + p_a^s\;sin(asx)\right)\left(p_b^c\;cos(bsy) + p_b^s\;sin(bsy)\right) \qquad (4)$$

where C and P terms are used for the core and holes respectively, $s = 2\pi/\ell$, ℓ is the transverse extent, and ψ_a^d is ψ_a^m with w_m replaced by w_d. Typically, the number of terms required for an accurate solution are $C = 20$ and $P = 200$. To simplify the analysis we expand $\ln(n^2)$ in the same way as n^2, since they have the same spatial distribution. The coefficients in the decompositions are evaluated by performing overlap integrals, which only need to be calculated once for any structure.

The decompositions defined above can be used to turn Eqs (2) into an eigenvalue problem. Using the decompositions, the vector wave equations can be written as

$$\begin{bmatrix} \mathcal{M}^{xx} & \mathcal{M}^{xy} \\ \mathcal{M}^{yx} & \mathcal{M}^{yy} \end{bmatrix} \hat{\mathbf{v}} = \frac{\beta^2}{k^2} \hat{\mathbf{v}} \tag{5}$$

where the components of $\hat{\mathbf{v}}$ are: $(\mathcal{E}^x_{00}, ...\mathcal{E}^x_{0\mathcal{F}}, \mathcal{E}^x_{10}, ...\mathcal{E}^x_{\mathcal{F}\mathcal{F}}, \mathcal{E}^y_{00}, ...\mathcal{E}^y_{0\mathcal{F}}, \mathcal{E}^y_{10}, ...\mathcal{E}^y_{\mathcal{F}\mathcal{F}})$ where $\mathcal{F} = F - 1$ for compactness. The matrices $\mathcal{M}^{ij}$ from Eqs (5) take the form

$$\begin{pmatrix} M^{ij}_{0000} & \cdots & M^{ij}_{000\mathcal{F}} & M^{ij}_{0010} & \cdots & M^{ij}_{00\mathcal{F}\mathcal{F}} \\ \vdots & \vdots & \vdots & \vdots & \vdots & \vdots \\ M^{ij}_{0\mathcal{F}00} & \cdots & M^{ij}_{0\mathcal{F}0\mathcal{F}} & M^{ij}_{0\mathcal{F}10} & \cdots & M^{ij}_{0\mathcal{F}\mathcal{F}\mathcal{F}} \\ M^{ij}_{1000} & \cdots & M^{ij}_{100\mathcal{F}} & M^{ij}_{1010} & \cdots & M^{ij}_{10\mathcal{F}\mathcal{F}} \\ \vdots & \vdots & \vdots & \vdots & \vdots & \vdots \\ M^{ij}_{\mathcal{F}\mathcal{F}00} & \cdots & M^{ij}_{\mathcal{F}\mathcal{F}0\mathcal{F}} & M^{ij}_{\mathcal{F}\mathcal{F}10} & \cdots & M^{ij}_{\mathcal{F}\mathcal{F}\mathcal{F}\mathcal{F}} \end{pmatrix} \tag{6}$$

where

$$M^{xx}_{abcd} = \frac{1}{k^2} I^{(1)}_{abcd} + I^{(2)}_{abcd} + \frac{1}{k^2} I^{(3)xx}_{abcd} \tag{7}$$

$$M^{xy}_{abcd} = \frac{1}{k^2} I^{(3)xy}_{abcd} \tag{8}$$

$$M^{yx}_{abcd} = \frac{1}{k^2} I^{(3)yx}_{abcd} \tag{9}$$

$$M^{yy}_{abcd} = \frac{1}{k^2} I^{(1)}_{abcd} + I^{(2)}_{abcd} + \frac{1}{k^2} I^{(3)yy}_{abcd} \tag{10}$$

and the I are overlap integrals of the modal functions, defined as

$$\begin{aligned} I^{(1)}_{abcd} &= \int_{-\infty}^{\infty}\int_{-\infty}^{\infty} \psi^m_a(x)\psi^m_b(y)\nabla^2\left[\psi^m_c(x)\psi^m_d(y)\right] dx\, dy \\ I^{(2)}_{abcd} &= \int_{-\infty}^{\infty}\int_{-\infty}^{\infty} n^2\psi^m_a(x)\psi^m_b(y)\psi^m_c(x)\psi^m_d(y)\, dx\, dy \\ I^{(3)ef}_{abcd} &= \int_{-\infty}^{\infty}\int_{-\infty}^{\infty} \psi^m_a(x)\psi^m_b(y)\frac{\partial}{\partial e}\left(\psi^m_c(x)\psi^m_d(y)\,\frac{\partial\left[\ln\left(n^2\right)\right]}{\partial f}\right) dx\, dy. \end{aligned} \tag{11}$$

These overlap integrals can all be evaluated analytically for the choice of decompositions made here, which is a significant advantage of this approach.

By solving Eqs (5) the modes and corresponding propagation constants of the fibre can be calculated. No assumptions need to be made about the polarisation of the guided modes. Solving the eigenvalue equation in Eq. 5 produces $2F^2$ eigenvalue/eigenvector pairs. Only one or a few of these pairs correspond to guided modes, and these modes can be distinguished by extracting the eigenvalues which fall within the range allowed by the structure (see Ref. [2]).

Using the model outlined here, the full range of possible *ideal* HF structures can be explored. In addition, the model can predict the properties of actual HFs. Typically, small imperfections in the hole arrangement arise during fabrication, and SEM photographs of real HF structures can be used to define the refractive index profile in the model [17]. This allows the deviations in optical properties which are caused by the subtle changes in structure to be explored for the first time.

CONCLUSIONS

A broad range of novel optical properties are possible in holey fibres, and these are largely determined by the air hole arrangement in the cladding. We have developed an efficient and accurate approach to modelling these structures which can provide insight into these properties. This model has been validated experimentally [6,17], and it is an important tool for the further development of this technology.

REFERENCES

1. T.A. Birks, J.C. Knight and P.St.J. Russell, Opt. Lett. **22**, 961 (1997).
2. T.M. Monro, D.J. Richardson, N.G.R. Broderick and P.J. Bennett, J. Lightwave Technol., **17**, 1093 (1999).
3. T.A. Birks, P.J. Roberts, P.St.J. Russell, D.M. Atkin and T.J. Shepherd, Elect. Lett. **31**, 1941 (1997).
4. R.F. Cregan, B.J. Mangan, J.C. Knight, T.A. Birks, P.St.J. Russell, P.J. Roberts and D.C. Allan, Science **285**, 1537 (1999).
5. T.M. Monro, P.J. Bennett, N.G.R. Broderick and D.J. Richardson, Opt. Lett. **25**, 206 (2000).
6. N.G.R. Broderick, T.M. Monro, P.J. Bennett and D.J. Richardson, Opt Lett. **24**, 1395 (1999).
7. J.C. Knight, T.A. Birks, R.F. Cregan, P.St.J. Russell and J.P. de Sandro, Elect. Lett. **34**, 1347 (1998).
8. T.M. Monro, D.J. Richardson, N.G.R. Broderick and P.J. Bennett, J. Lightwave Technol. **18**, 50 (2000).
9. T.M. Monro, D.J. Richardson and P.J. Bennett, Elect. Lett. **35**, 1188 (1999).
10. A. Ferrando, E. Silvestre, J.J. Miret, J.A. Monsoriu, M.V. Andrés and P.St.J. Russell, Elect. Lett. **35**, 325 (2000).
11. J.K Ranka, R.S. Windeler and A. Stentz, Opt. Lett. **25**, 796 (2000).
12. T.A. Birks, D. Mogilevtsev, J.C. Knight and P.St.J. Russell, IEEE Phot. Tech. Lett. **11**, 674 (1999).
13. E. Silvestre, M.V. Andrés and P. Andrés, J. Lightwave Technol., **16**, 923 (1998).
14. J.Broeng, S.E. Barkou, T. Sondergaard and A. Bjarklev, Opt. Lett. **25**, 96 (2000).
15. D. Mogilevtsev, T.A. Birks and P.St.J. Russell, Opt. Lett. **23**, 1662 (1998).
16. A. Snyder and J. Love, *Optical Waveguide Theory*, Chapman and Hall (1995).
17. P.J. Bennett, T.M. Monro and D.J. Richardson, Opt. Lett. **24**, 1203 (1999).